Stability of synchrony against local intermittent fluctuations in tree-like power grids

Sabine Auer, Frank Hellmann, Marie Krause, and Jürgen Kurths

Citation: Chaos **27**, 127003 (2017); doi: 10.1063/1.5001818
View online: https://doi.org/10.1063/1.5001818
View Table of Contents: http://aip.scitation.org/toc/cha/27/12
Published by the American Institute of Physics

Stability of synchrony against local intermittent fluctuations in tree-like power grids

Sabine Auer,[1,2,a)] Frank Hellmann,[1] Marie Krause,[3] and Jürgen Kurths[1,2,4,5]
[1]*Potsdam Institute for Climate Impact Research, 14412 Potsdam, Germany*
[2]*Department of Physics, Humboldt University Berlin, 12489 Berlin, Germany*
[3]*Institute of Mathematics, Technical University of Berlin, 10587 Berlin, Germany*
[4]*Department of Control Theory, Nizhny Novgorod State University, 606950 Nizhny Novgorod, Russia*
[5]*Institute of Complex Systems and Mathematical Biology, University of Aberdeen, Aberdeen AB24 3FX, United Kingdom*

(Received 24 February 2017; accepted 30 May 2017; published online 22 September 2017)

90% of all Renewable Energy Power in Germany is installed in tree-like distribution grids. Intermittent power fluctuations from such sources introduce new dynamics into the lower grid layers. At the same time, distributed resources will have to contribute to stabilize the grid against these fluctuations in the future. In this paper, we model a system of distributed resources as oscillators on a tree-like, lossy power grid and its ability to withstand desynchronization from localized intermittent renewable infeed. We find a remarkable interplay of the network structure and the position of the node at which the fluctuations are fed in. An important precondition for our findings is the presence of losses in distribution grids. Then, the most network central node splits the network into branches with different influence on network stability. Troublemakers, i.e., nodes at which fluctuations are especially exciting the grid, tend to be downstream branches with high net power outflow. For low coupling strength, we also find branches of nodes vulnerable to fluctuations anywhere in the network. These network regions can be predicted at high confidence using an eigenvector based network measure taking the turbulent nature of perturbations into account. While we focus here on tree-like networks, the observed effects also appear, albeit less pronounced, for weakly meshed grids. On the other hand, the observed effects disappear for lossless power grids often studied in the complex system literature. *Published by AIP Publishing.* [http://dx.doi.org/10.1063/1.5001818]

The full decarbonization of the energy sector by 2050 is non-negotiable to meet the emission targets of the Paris agreement.[1] Hence, the effort to deploy Renewable Energy Sources (RES) in the electricity, transport, and heat sectors continues and soon, the power system will undergo a regime shift from central conventional to distributed power production. For power grid operators this means: instead of centrally controlling and distributing large amounts of power from few power plants to the lower grid levels, the new challenge is to control lots of small generation units in a swarm-type manner. So far, the influence of the novel dynamics of intermittent power resources in these lower grid levels, called distribution grids, is poorly understood because there was no need to. However, the rapid approach of the regime shift asks for actions. This paper focuses on the stability of synchrony in distribution grids against local intermittent fluctuations at single nodes in the network and identifies network regions that are especially susceptible or infectious towards power fluctuations. Such insights will help to develop control techniques that are both feasible and cost-efficient.

I. INTRODUCTION

The increasing share of Renewable Energy Sources (RES) poses a wide range of challenges for power grid stability. Today, in Germany 90% of all installed power from RES lies in distribution grids.[2] With a growing number of especially wind and solar power plants, new dynamics are introduced into the lower grid layers which need to be understood. In the following, we investigate the influence of the power grid's topology and the placement of variable renewable infeed on stochastic stability measures in distribution grids. Our focus will be the stability of the synchronous state[3,4] and the ability of the system to keep frequency fluctuations small.

Work on the effect of stochastic fluctuations from RES on grid stability has been started very recently and thus, only few publications on this matter exist. For lossless power grids, the recent work[5] studied analytically the influence of single-node monochromatic oscillations and their spreading throughout the network. There, three frequency regimes were identified: a bulk, resonant, and local regime. In the bulk regime for low frequencies, the network is excited as a whole, whereas in contrast, high frequency perturbations stay localized at the fluctuating node and decay exponentially with the network distance. Most interestingly, for the mid-frequency region the network topology was identified to play a major role in network stability as complex, non-trivial patterns of stability and instability emerge. This analytical work is an important basis for understanding the influence of intermittent noise on power grid stability where fluctuations cover the whole frequency spectrum with a Kolmogorov-like turbulent power spectrum.[6–8]

a)auer@pik-potsdam.de

In Ref. 9, the impact of the detailed stochastic properties of the RES infeed was studied in great detail. There, the authors compared white Gaussian noise, Gaussian noise with a turbulent power spectrum, and intermittent noise. The latter noise displays a fat tail in both the power spectrum and the increment time series, which corresponds to a (long-range) correlation in time. The work showed that the time-correlated noise leads to the strongest network destabilization. Noise of the same power spectrum but without intermittency induces smaller frequency deviations. Thus, it is most important to include the intermittent nature of RES power fluctuations in future grid stability analysis.[5,9] the importance of the topology aspect has been already mentioned.[10] It was shown for two nodes (with white-noise power fluctuations) coupled to a bulk grid how the node with lower coupling strength is the one destabilizing the network. Moreover, with Kramer's escape rate theory the authors demonstrated how in a network with all machines subject to white noise, the weakest may be identified by the "saddles" of the grid which do not necessarily coincide with the most heavily loaded ones.

In contrast to previous studies, here we specifically model losses in the context of islanded microgrids[11] (see Sec. II) with intermittent fluctuations localized at a single node. Thereby, we focus on how the position of the perturbed node in the network influences its ability to corrupt the whole power grid system. Today distribution grids are part of a strongly hierarchical network structure and power is provided in a top-down manner from large, central production units. Here, we treat a different grid infrastructure, which is in line with the concept of self-sustaining grids that are balanced internally and thus, not connected to the upper grid level. This is one out of a few potential future concepts and at the same time, a very useful model to isolate the influence of the network structure on stability.

In this way, we can classify branches of nodes as troublemakers and fluctuation sensitive nodes. The net power outflow of each branch determines to what extent power fluctuations at associated nodes tend to cause notable frequency fluctuations at all network nodes. We call these nodes troublemakers or drivers of instability. The other classification describes nodes that react with notable frequency fluctuations irrespective of which node introduces the power fluctuations into the network. Such nodes appear especially pronounced for low coupling strength and can be identified with a novel network measure based on a turbulent weighting of the eigenvectors of the Jacobian.

In the following, we consider the model cases of an islanded microgrid described in Sec. II B together with a description of the intermittent noise in Sec. II C. In Sec. II D, we discuss adequate measures for stability in such a stochastic modeling setup. Finally, Sec. III presents the results which are discussed in Sec. IV.

II. MODEL SETUP

A. Distribution grid model

Our model is designed to represent distribution grids. Thus, we chose tree-shaped networks as the underlying topology (generated with a random growth model[12]) and introduce lossy lines, since the common assumption of non-lossy lines for transmission grids does not hold for distribution grids.

It is our objective to model a future islanded microgrid in a very conceptual way. To study the effect of local fluctuations on dynamic grid stability and isolate the influence of the network structure, we make the following model assumptions.

First, we assume a grid which is dominated by inverters because we want to analyze a scenario with high RES penetration where wind and solar power plants are connected to the grid via inverters. Nodes in our network are to be considered as effective nodes with a mix of at least one grid-forming inverter, a number of grid-feeding inverters, and demand.[11] In a future microgrid, we assume that for reasons of grid stability grid-forming inverters will be widely deployed. Because grid-feeding inverters do not contribute any inertia, our effective nodes have inertia much lower than nodes fully consisting of grid-forming inverters would have. Third, net generators and consumers are randomly and homogeneously distributed on the network. These modeling assumptions strive to strike a balance between realistic and conceptual.

The classical power grid model (or swing equation) is derived from the Synchronous Machine Model representing conventional generators and their rotating masses.[13] Inverters and their power electronics may be programmed as Virtual Synchronous Machines by using a smooth droop control. This then leads to the same equations for the voltage angle ϕ and frequency ω in terms of the (virtual) inertia H, power infeed P, (virtual) damping α, line susceptabilities, $Y = G + jB$, and voltage magnitudes U[14]

$$\begin{aligned}\dot{\phi}_i &= \omega_i,\\ \dot{\omega}_i &= \frac{1}{H}\Bigg(P_i + \Delta P(t)\delta_{ik} - \alpha\omega_i \\ &\quad - \sum_j U_i|Y_{ij}|U_j \sin\left(\phi_i - \phi_j + \phi_{ij}\right)\Bigg).\end{aligned} \tag{1}$$

The virtual inertia and damping for the network model are given by the low-pass filter exponent τ_p and the droop control parameter k_p from grid-forming inverters: $H = \tau_p/k_p$, $\alpha = 1/k_p$, $\forall\ i$ with $i = 1,\ldots,N$. Standard parameters for the droop and time constants of grid-forming inverters are in the range $k_p = [0.1,\ldots,10]s^{-1}$ and $\tau_p = [0.1,\ldots,10]s$.[14,15] At the upper boundary of both parameter ranges, this would result in $\alpha = 0.1\,s$ and $H = 1s^2$. However, here we assumed a low-inertia and low-damped system represented by a mix of grid-forming and grid-feeding inverters (with zero inertia) and thus, we decrease both values by one scale: $\alpha = 0.01\,s$ and $H = 0.1s^2$. While low inertia and damping make the observed phenomena more pronounced, they do not qualitatively change the behavior of the system, especially with respect to the network topology's influence. The power fluctuation $\Delta P(t)$ is only applied at node k. The impedance of the lines for typical Mid-Voltage grid lines with 20 kV base voltage equals $Z = Y^{-1} = (0.4 + 0.3j)\Omega/\mathrm{km}\cdot l$.[16] The coupling strength K_{ij} between a node pair (i, j) then equals

$$K_{ij} = U_i|Y_{ij}|U_j, \tag{2}$$

where $|U_i| = 20$ kV. For simplicity all power, voltage, and impedance values are transformed into per unit with a base

voltage of 20 kV and a base power of 1 MW, which are typical values for MV grids.[16,17] The absolute impedance of each line scales with the geographic distance l between linked nodes and is consequently different among the links. The average line length, according to Ref. 16, is 23.7 km. The addition of the resistance leads to line losses and at the same time introduces a phase shift of $\phi_{ij} \approx \arctan\left(\frac{G_{ij}}{B_{ij}}\right)$ that does not occur in the non-lossy model but will be shown to have significant consequences for stability. The Jacobian of (1) equals

$$\mathbf{J} = \begin{bmatrix} \frac{\partial \dot{\phi}_i}{\partial \phi_j} & \frac{\partial \dot{\phi}_i}{\partial \omega_j} \\ \frac{\partial \dot{\omega}_i}{\partial \phi_j} & \frac{\partial \dot{\omega}_i}{\partial \omega_j} \end{bmatrix}. \tag{3}$$

For each simulation run, the same intermittent time series (the sum of wind and solar power fluctuations, scaled with the power production) was added to a single node's power input.

The equation is written in a co-rotating frame; thus, the synchronous state we study is characterized by $\omega_i = 0$. Hence, we are interested in the deviations from the stable frequency set point which corresponds to 50 Hz. In the following, we mainly investigate $\Delta f = \omega/(2\pi)$.

B. Microgrids as a model case

In order to understand the abillity of a distributed system to maintain synchrony, we will study the case of an islanded microgrid that is internally balanced and not connected to a higher grid level. Islanded microgrids play a role in the decentral provision of energy, but also as part of a safety and stability strategy to localize faults by partitioning the grid into autonomous units.

A microgrid has a non-hierarchical grid topology. The grid is balanced within itself, in our case there are 50 net producers and 50 net consumers with $P_i = \pm 0.2$ MW power infeed before losses. The power infeeds are chosen homogeneously to isolate topology and network effects in the model. As there is no connection to upper grid levels, losses are compensated locally at each node, and the net power infeed is given by $\tilde{P}_i = (P_i + P_{loss}/N)$. To compensate losses locally, in the fix point search a loss compensator term was added to each node's power input which ensures that the system frequency does not deviate from 50 Hz.

C. Intermittent noise

In the following simulations, the intermittent time series for solar and wind power fluctuations were generated by a clear sky index model, based on a combination of a Langevin and a Jump process, developed in Ref. 8, and a Non-Markovian Langevin type model developed in Ref. 9, respectively. An example time series, $\Delta P(t)$, of the combined wind and solar power fluctuations, $\Delta P_W(t)$ and $\Delta P_S(t)$, respectively, is shown in Fig. 1 (left)

$$\Delta P(t) = 0.5\Delta P_W(t) + 0.5\Delta P_S(t). \tag{4}$$

The stochastic nature of such processes was identified in Refs. 8 and 9 with the help of time series analysis. Important characteristics are the probability distribution function (PDF), the increment distribution, and the power spectrum. If the PDFs, of both the time series of power and power increments, are fat tailed (the tails are not exponentially bounded[18]), we define this as intermittency. Also, the power generation from wind and solar power plants has a power spectrum that is power-lawed with the Kolmogorov exponent of turbulence.[6,8] Thus, time series from such sources show long-term temporal correlations. The Hurst exponent $0 < h < 1.0$ is a time-lag dependent measure for such long-time memory in a time series.[19–22] It quantifies the rate at which the autocorrelations

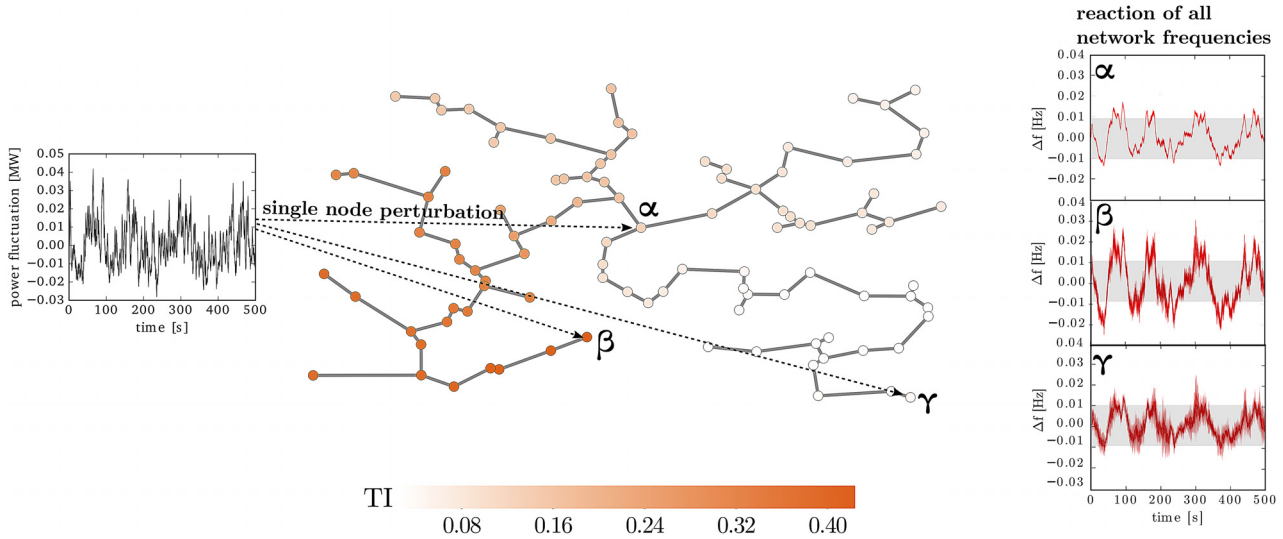

FIG. 1. Left: Power fluctuation time series $\Delta P(t)$ jointly generated by solar and wind models that capture their intermittent behavior.[8,9] Center: Random microgrid with *TI* as colouring. One simulation run with single node fluctuations at one specific node produces this node's *TI* value Right: Frequency time series for all network nodes $T = 500$ s for single-node fluctuations at node α, β, and γ. The grey zone is the frequency threshold band of 0.01 Hz. All 100 nodes' frequency trajectories are shown with semi-transparent red lines.

of the time series decreases with increasing time lag. In this work, we display the turbulent and intermittent nature of RES with long-term positive autocorrelation h close to unity and fat-tailed increment distributions.

D. Stochastic stability measures

The stability measures typically used in power grid synchronization analysis are not applicable to our stochastic system.[23–28] Instead, we use the *exceedance* as our main stochastic stability measure to quantify the stability of the synchronous state. It is the cumulated time an observable stays outside a defined "safe" region. For our case, we define a frequency threshold of 0.01 Hz. This threshold corresponds to the so-called dead band from the German transmission code which defines at which frequency primary control actions kick in to balance deviations from the desired 50 Hz set point.[29]

As we apply single-node fluctuations (see Fig. 1) for each run, $i = 1,\ldots,N$, and record the frequency response for each node $j = 1,\ldots,N$, we end up with $N \times N$ frequency time series from which stability measures are derived. In the colorplot of Fig. 2, the single node exceedance, $E_{i,j}$, is plotted. One grid value represents the probability of network node j to be outside the given frequency band when node i is perturbed

$$E_{i,j} = P_i(|f_j| > 0.01). \tag{5}$$

This can be further aggregated into the following nodal measures:

- The average exceedance over all N nodes given a perturbation at i, which we call *Troublemaker Index (TI)*:

$$\bar{E}_i = \frac{1}{N}\sum_{j=1}^{N} E_{i,j}. \tag{6}$$

  Power fluctuations at a node with a high *TI* causes large frequency deviations often and/or at many nodes.
- *Excitability* quantifies how much a single-node is exceeding the frequency threshold on average when a random node in the network is perturbed:

$$\bar{E}_j = \frac{1}{N}\sum_{i=1}^{N} E_{i,j}. \tag{7}$$

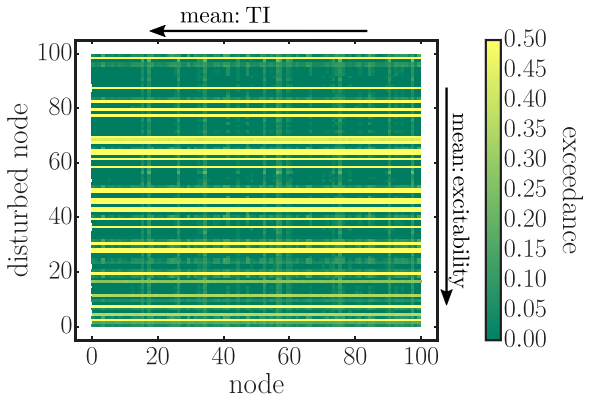

FIG. 2. Color Plot of Single Node Exceedances [see (5)] for each simulation run or disturbed node (y-axis) and each node in the network (x-axis) for a lossy microgrid ($Z = (0.4 + 0.3j)$ Ω/km l, where l is the link length).

  Nodes with high excitability react strongly for many origins of the perturbation within the network. We call such nodes highly sensitive.

Further, we study the *time average of frequency dispersion (TAFD)*, the spread in frequency values among between the network nodes averaged over the simulation time

$$TAFD = \frac{1}{T}\sum_{t=0}^{T}\left[\frac{1}{N}\sum_{i}^{N}(\Delta f_{i,t} - \mu_t)^2\right], \tag{8}$$

where $\Delta f_{i,t}$ is the ith node's frequency deviation and μ_t is the mean frequency deviation, averaged over all nodes, at time t. This is a direct measure of the inhomogeneity introduced by the localized fluctuations.

And as a measure for temporal correlations we recorded the Hurst exponent $h_{i,t}$ (the Hurst exponent for the frequency time series of node j with fluctuation power input at node i). The single node influence of node i on the mean Hurst exponent of the whole grid was calculated as

$$h_i = \frac{1}{N}\sum_{j=1}^{N} h_{i,j}. \tag{9}$$

III. RESULTS

In one simulation run, single-node fluctuations are introduced for one specific node. For better comparability, the same fluctuation time series is used for each node. Then, the reaction of the whole network towards such fluctuations at the certain node position in the network is investigated. We find a remarkable interplay of the network structure and the position of the node at which the fluctuations are fed in.

A first important result is that this interplay and the dependence on the position of nodes, at which power infeed is fluctuating, only appear due to the losses in distribution grids. A strongly coupled lossless grid reacts as one and identically to perturbations, no matter where they occur, the exceedance plot is homogeneous. The network and position of the perturbation play no role here. As can be seen in Fig. 3, a lossless grid with relatively weak lines will lead to strongly and weakly interacting nodes. In any pair of nodes i, j, the reaction of node i to perturbations at node j is identical to the reaction of j to perturbations at i. The exceedance plot is symmetric in this case. However, the differences in exceedance remain relatively small, even in this case.

Generally, losses increase the absolute value of and the differences in exceedance. Also, only with losses present do specific troublemakers appear (see Fig. 2).

The importance of losses is a main result of this paper; however we have no sound explanation for this, so far. Here, we expect the work of Ref. 5 to provide an avenue towards an analytical understanding. Details will be left to follow-up work. Nevertheless, a model setup without lossy lines would miss the following insights.

The rest of this section will discuss in detail the relationship of various network structures and dynamical properties. Our main findings in short are the following:

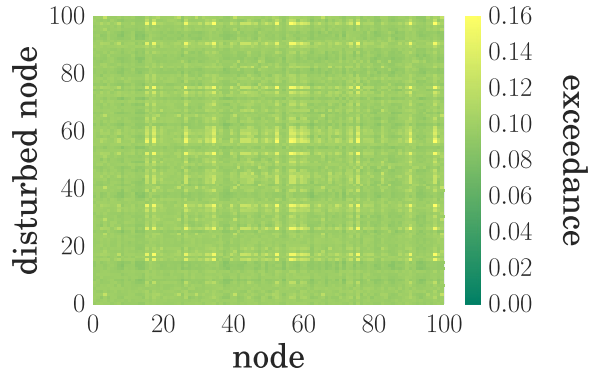

FIG. 3. Color Plot of Single Node Exceedances [see (5)] for each simulation run or disturbed node (y-axis) and each node in the network (x-axis) with 10% coupling strength (see K_{ij} in (2)) and non-lossy lines ($Z = (0 + 0.3j)\ \Omega$/km l with link length l). The same plot for a 100% coupling strength leads to $E_{ij} \approx 0.16\,\forall i, j$.

We find network branches with different stability behavior. The top row of Fig. 4 shows branches of troublemakers (with relatively high *TI*) and branches of vulnerable nodes (with relatively high excitability). The bottom row of Fig. 4 additionally tells us that *TI* and the mean Hurst exponent are strongly correlated. Thus, nodes causing frequency fluctuations above threshold in the whole grid are exactly those that are able to maintain temporal correlations in the frequency time series, $\Delta f_i(t)$, over all grid nodes i.

At the same time, nodes reacting strongly to intermittent power infeed, $\Delta P(t)$, at whatever node in the grid, themselves, show little ability to be drivers of exceedance. Instead, fluctuations at such nodes lead to large frequency incoherencies or frequency spread (*TAFD*) among the nodes. Hence, high TI does not necessarily mean high frequency spread and vice versa. Nodes, that destabilize the grid, causing large fluctuations at all nodes, are not the same nodes that make the grid incoherent. On the other hand, high *TI* nodes are the same nodes that pass on temporal correlations to the other grid nodes.

After these first insights, we want to develop a better understanding of how network structure and high values of *TI* and excitability are related in Secs. III A and III B, respectively.

A. The curious tale of troublemakers

From the time series plots in Fig. 1 (right), it can be seen that it makes a difference in the evolution of frequency deviation on what node the power fluctuations are exerted. The distribution of *TI* over the network (Fig. 1 center) shows how nodes of the same branch behave coherently, they have similar capabilities to be drivers of instability. The frequency time series $\Delta f(t)$ of all network nodes further illustrates the different reaction of the network towards power fluctuations $\Delta P(t)$ at single nodes (see Fig. 1 right). Here, two dead-end nodes from different branches (nodes β and γ) and a node connecting branches, the most closeness central node α, were chosen. We see that node β is a troublemaker by exceeding the frequency threshold most. α and γ exceed less, however, with quite different *TAFD* values. The emergence of *TI* values different for each branch in the network is remarkable because even for a microgrid with homogeneous power distribution the network topology seems to play an important role.

From Fig. 5 (left), a clear but non-trivial relationship between *TI* and closeness centrality is visible. The closeness centrality, cc_i, of node i is defined as the inverse sum over all shortest paths between node i and all other nodes j of the network.[30] Therefore, a large cc value characterizes a node with short distances to all other nodes of the network. Connecting

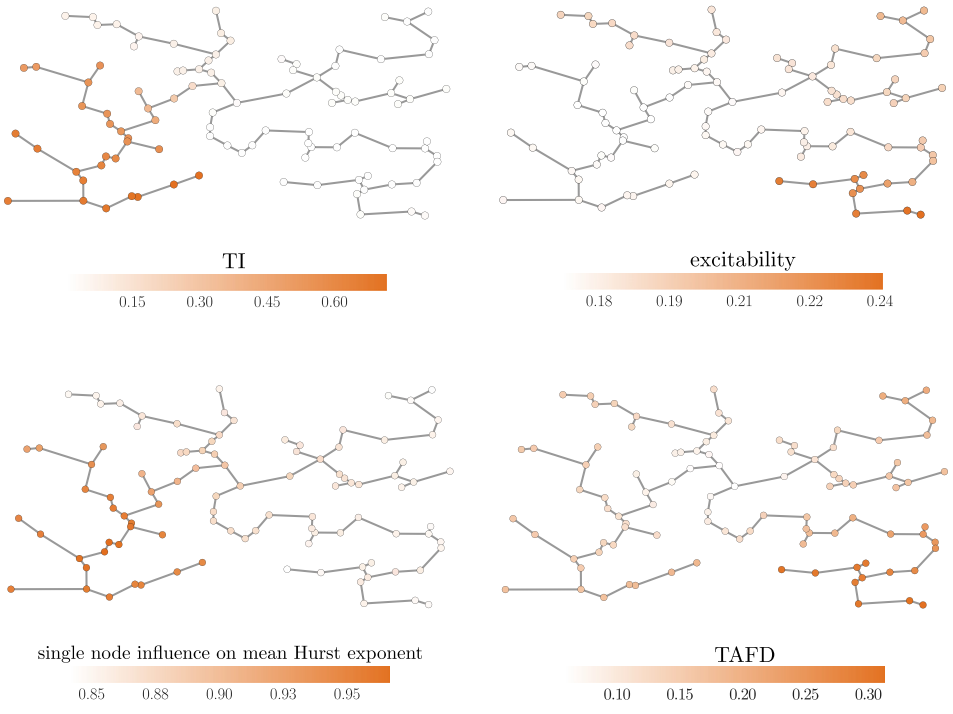

FIG. 4. Top left: The Troublemaker Index [*TI*, see (6)] as the mean over the x-axis of the colorplot. Top right: Excitability [see (7)] is the mean over the y-axis of the colorplot. Bottom left: Network plot of single node influence on mean Hurst exponent, see (9). Bottom right: Time average of grid's frequency spread [*TAFD*, see (8)], normalized to average mean deviation) as coloring.

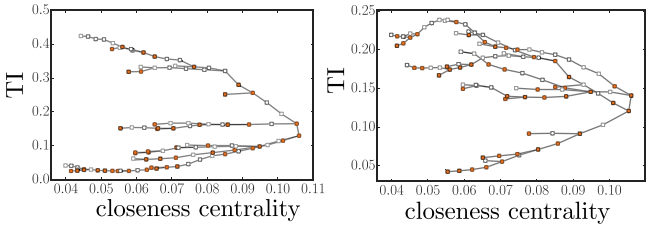

FIG. 5. *TI* over closeness centrality, *cc*, for coupling strength for different power input configurations (different realizations of the distribution of net consumers and producers) on the same distribution grid. White and orange nodes represent net consumers and producers, respectively.

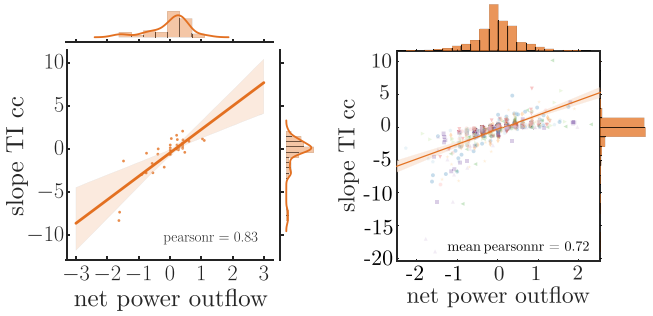

FIG. 6. Slope of *TI* over closeness centrality, *cc* [see (10)] on the x-axis and branch net power outflow, $P_{out,i}$ [see (11)] for one example grid (left) different distribution grid topologies (right).

nodes adjacent to each other in the *TI*(*cc*)-plot gives additional information. It underlines how branches of high *TI* are actual physical network branches. The highest centrality node separates the network into branches of troublemaker nodes and low *TI* branches (see Figs. 5 and 6). Hence, certain but not all nodes lead to a temporary desynchronization, even if the frequency is mostly in the bulk regime (see Fig. 7). However, why network branches are shifted by different constant factors in *TI* is not clear at first sight and is investigated in the following.

From Fig. 5, it becomes evident that different power input configurations play a central role in this phenomenon because a change in the power input configuration alters the branches' *TI* values. The appearance of net consumers or producers along the lines towards its dead ends seems to increase or decrease *TI*, respectively. Due to the losses that are compensated by an equal extra production by all nodes, there is a small asymmetry between net consumer and producer power inputs.

Nevertheless, Fig. 5 shows how branches split up with varying slopes for decreasing closeness centrality (*cc*). Hence, a relationship between the *TI*–*cc*-slope and branch net power outflow can be established. In Fig. 6 (left), this relationship is plotted for one example grid. The *TI*–*cc*-slope is calculated for branch parts as

$$slope_{i,j} = \frac{TI_j - TI_i}{cc_j - cc_i}, \tag{10}$$

which lie between two node pairs (i, j) with degree $k \geq 3$ because starting from the most closeness central node each branching seems to alter the slope. This slope is then compared with the net power outflow

$$P_{out,i} = \sum_{k \in B_i} P_k \tag{11}$$

or the sum over all power inputs of all nodes between the branch part node i with highest *cc* in the branch and all other branch nodes, k, which are elements of the node set B_i with $cc_k < cc_i$. Figure 6 shows how small slopes are well correlated with net power outflow but we also find especially large slopes which belong to branch parts closer to the most closest central node. Nevertheless, the Pearson correlation coefficient is 0.83 for the example grid and on average equals 0.73 for an ensemble of 30 distribution grids. Also, the rule is always: branches with negative net power outflow above small values always have negative slopes and vice versa.

In a follow-up work, we aim for an analytical understanding of this phenomenon.

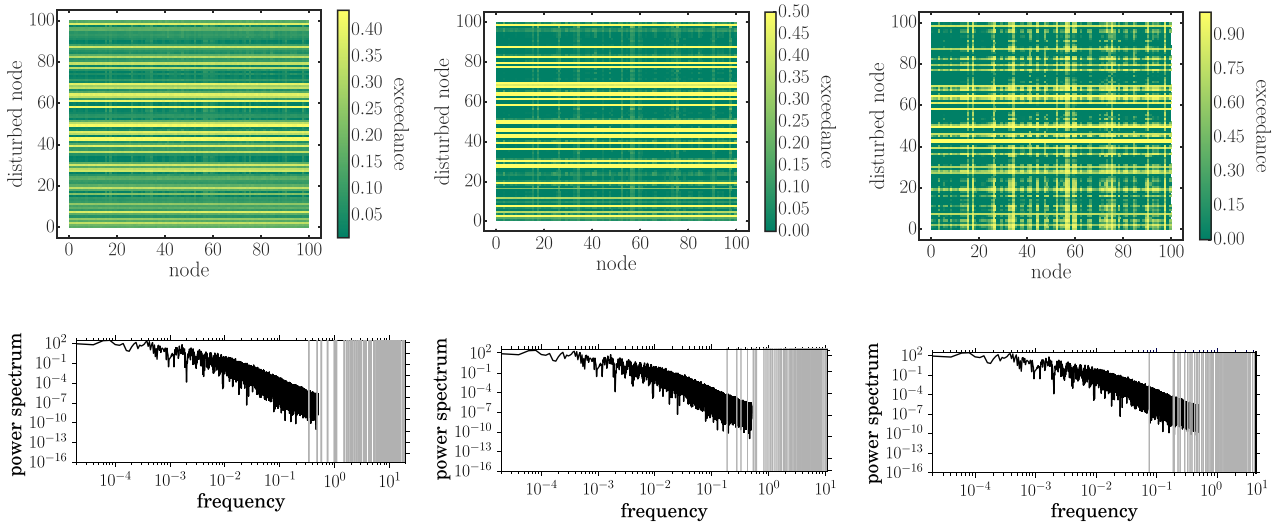

FIG. 7. Top row: Color plot, with disturbed node on the y-axis and reacting nodes of the network on the x-axis, of single node exceedance. Bottom row: power spectrum of power fluctuations (black) with network eigenfrequencies (dark blue vertical lines). From left to right: coupling strength in (1) scaled with factor 1.0, 0.3, and 0.1.

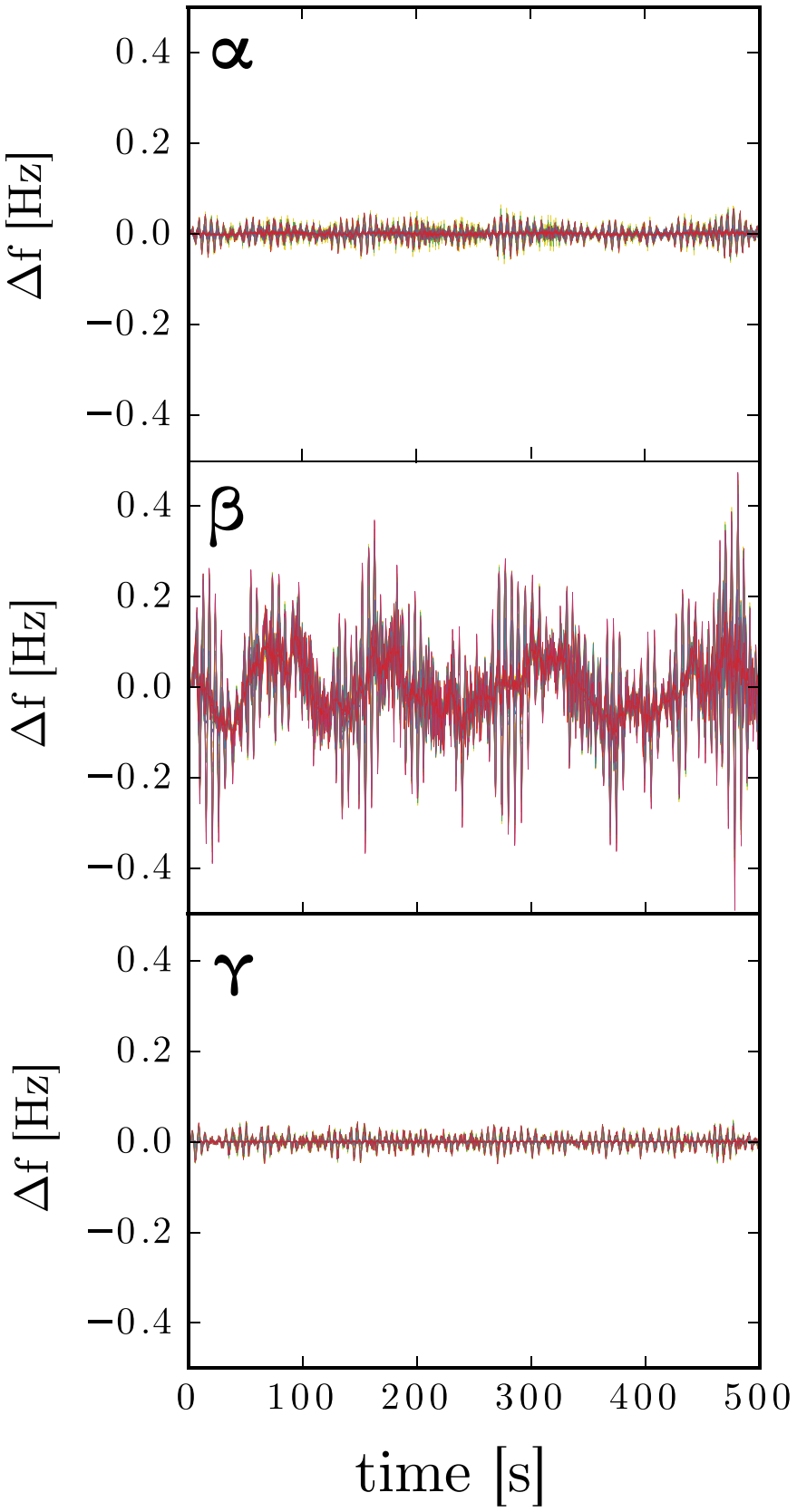

FIG. 8. Frequency time series for all network nodes for disturbances at node α, β, and γ. with coupling strength K_{ij} of (2) reduced to 10% compared to Fig. 1 of the same distribution grid with identical power input configuration. All 100 nodes' frequency trajectories are shown with different coloring.

B. High excitability and network eigenmodes

At first sight, equally reducing the coupling strength leads to a much more difference for exerting single-node perturbations to different nodes concerning the network frequency time series (see Fig. 8). For comparison, the same nodes as in Fig. 1 were chosen. Compared to nodes α and γ, the frequency fluctuations of node β are enormously high. For sure, node β is a troublemaker because fluctuations at this node lead to all network nodes to be on average 90% outside the given

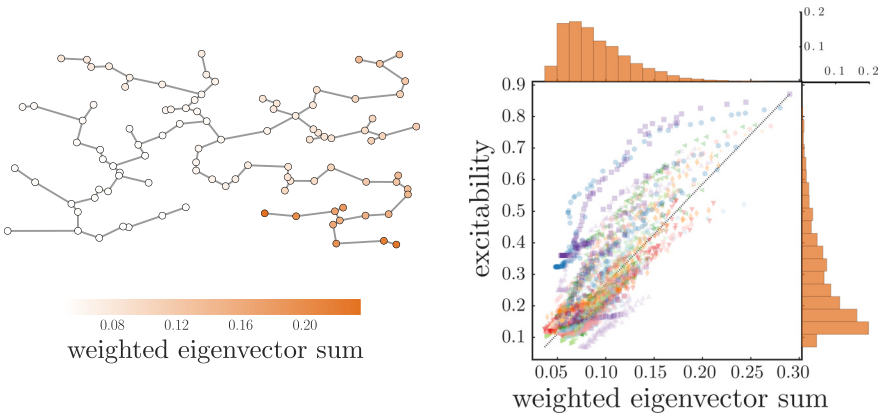

FIG. 9. Left: The sum of the weighted absolute values of the Jacobian eigenvectors for one example network. Right: Scatter plot of excitability over the weighted Jacobian's eigenvector sum for 30 randomly generated distribution grid trees. All networks have low coupling strength (scaled with factor 0.1) and each color represents one grid.

frequency band (*TI* value of 0.9). However, this node has been known as a troublemaker before, for higher coupling strength.

The color plots of Fig. 7 illustrate how the reduction of coupling strength also brings another aspect into play. For high coupling strength, it is clearly visible how some nodes are the driver of high single node exceedance values for all nodes in the network. Now, lowering coupling strength results in two node classes. For low coupling strength, there are drivers of instability and nodes that generally tend to be unstable irrespective of which node was initially perturbed. This is underlined by the excitability network plot of Fig. 1. Even without losses, in Fig. 3 we see such excitable nodes for low coupling strength. However, here troublemakers correspond to excitable nodes because the single-node exceedance is symmetric.

This is particularly interesting taking into account the power spectrum of the power fluctuations from wind and solar generation and comparing these with the eigenfrequencies of the Jacobian (see J_{ij} of (3)) of the distribution grid dynamics. Lowering coupling strength then shifts more and more eigenfrequencies into the power spectrum range of the power fluctuations (see bottom row of Fig. 7). Thus, the fluctuations more and more hit the so-called resonant regime mentioned in Ref. 5.

The generally instable nodes, appearing as vertical yellow lines in Fig. 7 (top right), are the nodes with large entries in the Jacobian's eigenvectors. This provides an analytical predictor for this phenomenon (see Fig. 9 (left) for a specific distribution grid tree and Fig. 9 (right) for an ensemble of networks). To take into consideration how strong certain eigenmodes of the system can be excited by the power spectrum of the induced fluctuations, we take a weighted sum (weight is the eigenfrequency to the power of –5/3, the Kolmogorov exponent from turbulence theory) of the Jacobian's eigenvectors $\mathbf{v}^j$ with entries v_k^j

$$\lambda^j v_k^j = \sum_{k'=1}^{2N} J_{kk'} v_{k'}^j. \tag{12}$$

We then obtain a measure on the network by summing over the entries associated with a particular node. The elements of this vector $\mathbf{V}^w$, written as V_m^w with $m = \{1, .., N\}$, are given by

$$V_m^w = \sum_{j=1}^{2N} |\Im(\lambda^j)|^{-5/3} \left(|v_m^j| + |v_{m+N}^j| \right), \tag{13}$$

where $\Im(\lambda^j)$ are the Jacobian's eigenfrequency values and $|v_m^j|$ is the absolute value of the mth entry of the Jacobian's jth eigenvector.

Concerning the Hurst exponent, it is symmetric towards the perturbed and reacting nodes. This means that correlation in time is preserved for certain nodes irrespective of what node is perturbed initially. The cross correlation between the time series of the disturbed node and all other nodes for different coupling strengths shows how for larger coupling strength cross correlation is generally higher than for networks with lower coupling strength.

IV. DISCUSSION

In this work, we showed how important the network position of single-node fluctuations is in terms of its influence on the overall stochastic grid stability. We found a remarkable and subtle but robust interplay of dynamical and topological properties, even in our case of a microgrid with a homogeneous distribution of identical net consumers and producers. This interplay is largely absent for lossless grids. Without the correct representation of distribution grids as lossy networks, this effect would therefore have stayed undiscovered. A sound analytical understanding of the importance of losses is an open problem and will be part of future work.

Drivers of instability, the so-called troublemakers, and fluctuation sensitive nodes appear on branches, which demonstrated coherent behavior within themselves. The most closeness central node has proven to play a special in role in this type of investigation because it splits the network in branches of such different behavior. The nature of troublemakers is based on a combination of the net power outflow of their corresponding branch part combined with their network centrality. Thus, different power input configurations lead to different results. Also, drivers of instability tend to pass on the temporal correlation of the intermittent power time series to the other grid nodes.

At the same time, at low coupling strength generally fluctuation sensitive nodes emerge. Such nodes of high excitability themselves have little capability to act as troublemakers. Instead they cause large frequency incoherencies. The reason for their appearance is a strong overlap of the network's

eigenfrequencies and the power fluctuation power spectrum for low coupling strength. This leads to large entries in the corresponding Kolmogorov weighted Jacobian's eigenvectors sum that enables us to identify the most excitable or fluctuation sensitive nodes. This gives us an analytical predictor which network regions are especially effected.

Despite our conceptual modeling approach, we would like to be make a few careful distribution grid design recommendations. As the issue of excitable nodes in lossy grids increases with reduced coupling strength, long lines and cables are especially affected and thus, are to be avoided in distribution grids. Also, the issue of troublemakers can be overcome with low resistance lines. However, the placement of RES at nodes that are no troublemakers, if possible, would be the cheapest solution. The potential use of adding new links to distribution grid trees, as a possible solution to increase grid stability, will be part of future work.

In future work, we want to improve our analytical understanding of how the network structure determines troublemakers. Also, a study on multiple node fluctuations will follow which asks for a better understanding of the spatial correlation between fluctuations in renewable energy production. To capture the effect of future voltage issues, as a next step we will introduce voltage dynamics in our power grid simulation.

From first simulation results, we could see that also meshed grids show the previously described effects, only less pronounced and with reduced values in exceedance. This means that our findings are not restricted to pure tree-like networks. Still, more detailed investigations of meshed grids, where the identification of branches for evaluation is not possible anymore, shall follow. At the same, such study poses the question how the smart placement of few additional lines may eliminate troublemakers.

There is little known about the influence of RES on frequency dynamics in distribution grids. However, results of our and related work help to reduce balancing needs and improve the placement of network stabilizing power balancers and cost-efficient control techniques.

ACKNOWLEDGMENTS

S.A. wants to thank her fellow colleagues Paul Schultz and Jobst Heitzig for helpful discussion and comments. The authors gratefully acknowledge the support of BMBF, CoNDyNet, FK. 03SF0472A and the European Regional Development Fund (ERDF), the German Federal Ministry of Education and Research and the Land Brandenburg for supporting this project by providing resources on the high performance computer system at the Potsdam Institute for Climate Impact Research.

[1]J. Rogelj, M. Den Elzen, N. Höhne, T. Fransen, H. Fekete, H. Winkler, R. Schaeffer, F. Sha, K. Riahi, and M. Meinshausen, "Paris agreement climate proposals need a boost to keep warming well below 2 c," Nature **534**(7609), 631–639 (2016).

[2]See https://www.bmwi.de/Redaktion/EN/Publikationen/verteilernetzstudie.pdf?__blob=publicationFile&v=1 for Study for the Federal Ministry of Economics and Technology (BMWi). Moderne verteilernetze für deutschland (verteilernetzstudie).

[3]A. Arenas, A. Díaz-Guilera, J. Kurths, Y. Moreno, and C. Zhou, "Synchronization in complex networks," Phys. Rep. **469**(3), 93–153 (2008).

[4]F. Dörfler and F. Bullo, "Synchronization in complex networks of phase oscillators: A survey," Automatica **50**(6), 1539–1564 (2014).

[5]X. Zhang, S. Hallerberg, M. Matthiae, D. Witthaut, and M. Timme, "Dynamic network response patterns," Dyn. Network Res. Patterns (unpublished).

[6]P. Milan, M. Wächter, and J. Peinke, "Turbulent character of wind energy," Phys. Rev. Lett. **110**(13), 138701 (2013).

[7]A. Woyte, R. Belmans, and J. Nijs, "Fluctuations in instantaneous clearness index: Analysis and statistics," Sol. Energy **81**(2), 195–206 (2007).

[8]M. Anvari, G. Lohmann, M. Wächter, P. Milan, E. Lorenz, D. Heinemann, M. Reza Rahimi Tabar, and J. Peinke, "Short term fluctuations of wind and solar power systems," New J. Phys. **18**(6), 063027 (2016).

[9]J. Peinke, K. Schmietendorf, and O. Kamps, "On the stability and quality of power grids subjected to intermittent feed-in," preprint arXiv:1611.08235 [nlin.AO] (2016).

[10]B. Schäfer, M. Matthiae, X. Zhang, M. Rohden, M. Timme, and D. Witthaut, "Escape routes, weak links, and desynchronization in fluctuation-driven networks," Phys. Rev. E **95**, 060203 (2017).

[11]J. Schiffer, D. Zonetti, R. Ortega, A. M. Stanković, T. Sezi, and J. Raisch, "A survey on modeling of microgrids –from fundamental physics to phasors and voltage sources," Automatica **74**, 135–150 (2016).

[12]P. Schultz, J. Heitzig, and J. Kurths, "A random growth model for power grids and other spatially embedded infrastructure networks," Eur. Phys. J. Spec. Top. **223**(12), 2593–2610 (2014).

[13]T. Nishikawa and A. E. Motter, "Comparative analysis of existing models for power-grid synchronization," New J. Phys. **17**(1), 015012 (2015).

[14]S. Johannes, G. Darina, R. Jorg, and S. Tevfik, "Synchronization of droop-controlled microgrids with distributed rotational and electronic generation," in *2013 IEEE 52nd Annual Conference on Decision and Control (CDC)* (IEEE, 2013), pp. 2334–2339.

[15]E. A. A. Coelho, P. C. Cortizo, and P. F. D. Garcia, "Small-signal stability for parallel-connected inverters in stand-alone ac supply systems," IEEE Trans. Ind. Appl. **38**(2), 533–542 (2002).

[16]A. Sabine, S. Florian, C. Wang, S. Andrei, and S. Rudolf, and "Can distribution grids significantly contribute to transmission grids' voltage management?," In *2016 IEEE PES Innovative Smart Grid Technologies Conference Europe (ISGT-Europe)* (IEEE, 2016), pp. 1–6.

[17]P. C. Sen, *Principles of Electric Machines and Power Electronics* (John Wiley & Sons, 2007).

[18]S. Asmussen, *Applied Probability and Queues* (Springer Science & Business Media, 2008), Vol. 51.

[19]H. E. Hurst, "The problem of long-term storage in reservoirs," Hydrol. Sci. J. **1**(3), 13–27 (1956).

[20]E. Alessio, A. Carbone, G. Castelli, and V. Frappietro, "Second-order moving average and scaling of stochastic time series," Eur. Phys. J. B-Condens. Matter Complex Syst. **27**(2), 197–200 (2002).

[21]T. Preis, P. Virnau, W. Paul, and J. J. Schneider, "Accelerated fluctuation analysis by graphic cards and complex pattern formation in financial markets," New J. Phys. **11**(9), 093024 (2009).

[22]A. Carbone, G. Castelli, and H. E. Stanley, "Analysis of clusters formed by the moving average of a long-range correlated time series," Phys. Rev. E **69**(2), 026105 (2004).

[23]F. Hellmann, P. Schultz, C. Grabow, J. Heitzig, and K. Jürgen, "Survivability: A unifiying concept for the transient resilience of deterministic dynamical systems," Nature Scientific Reports 6(29654) (2016).

[24]P. J. Menck, J. Heitzig, N. Marwan, and J. Kurths, "How basin stability complements the linear-stability paradigm," Nat. Phys. **9**(2), 89–92 (2013).

[25]T. Nishikawa and A. E. Motter, "Synchronization is optimal in nondiagonalizable networks," Phys. Rev. E **73**(6), 065106 (2006).

[26]L. M. Pecora and T. L. Carroll, "Master stability functions for synchronized coupled systems," Phys. Rev. Lett. **80**(10), 2109 (1998).

[27]V. N. Belykh, I. V. Belykh, and M. Hasler, "Connection graph stability method for synchronized coupled chaotic systems," Phys. D: Nonlinear Phenom. **195**(1), 159–187 (2004).

[28]S. Auer, K. Kleis, P. Schultz, J. Kurths, and F. Hellmann, "The impact of model detail on power grid resilience measures," Eur. Phys. J. Spec. Top. **225**(3), 609–625 (2016).

[29]Verband der Netzbetreiber, See https://www.bdew.de/internet.nsf/id/A2A0475F2FAE8F44C12578300047C92F/$file/TransmissionCode2007.pdf for Transmissioncode (2007).

[30]M. E. J. Newman, "The structure and function of complex networks," SIAM Rev. **45**(2), 167–256 (2003).